

MASS SPECTRUM OF THE AXIAL-VECTOR HIDDEN CHARMED AND HIDDEN BOTTOM TETRAQUARK STATES

Zhi-Gang Wang¹

Department of Physics, North China Electric Power University, Baoding 071003, P. R.
China

Abstract

In this article, we perform a systematic study of the mass spectrum of the axial-vector hidden charmed and hidden bottom tetraquark states using the QCD sum rules, and identify the $Z^+(4430)$ as an axial-vector tetraquark state tentatively.

PACS number: 12.39.Mk, 12.38.Lg

Key words: Tetraquark state, QCD sum rules

1 Introduction

The Babar, Belle, CLEO, D0, CDF and FOCUS collaborations have discovered (or confirmed) a large number of charmonium-like states, such as $X(3940)$, $X(3872)$, $Y(4260)$, $Y(4008)$, $Y(3940)$, $Y(4325)$, $Y(4360)$, $Y(4660)$, etc, and revitalized the interest in the spectroscopy of the charmonium states [1, 2, 3, 4, 5, 6]². Many possible assignments for those states have been suggested, such as multiquark states (irrespective of the molecule type and the diquark-antidiquark type), hybrid states, etc [1, 2, 3, 4, 5].

The $Z^+(4430)$ observed in the decay mode $\psi'\pi^+$ ($B \rightarrow \psi'\pi^+K$) by the Belle collaboration is the most interesting subject [7, 8]. We can distinguish the multiquark states from the hybrids or charmonia with the criterion of non-zero charge. The $Z^+(4430)$ can't be a pure $c\bar{c}$ state due to the positive charge, and may be a $c\bar{c}u\bar{d}$ tetraquark state. However, the Babar collaboration did not confirm this resonance [9]. Furthermore, the two resonance-like structures $Z(4050)$ and $Z(4250)$ in the $\pi^+\chi_{c1}$ invariant mass distribution near 4.1 GeV are also particularly interesting [10]. Their quark contents must be some special combinations of the $c\bar{c}u\bar{d}$, just like the $Z^+(4430)$, they can't be the conventional mesons. There have been several theoretical interpretations for the $Z^+(4430)$, such as the hadro-charmonium resonance [3, 11], the S -wave threshold effect [12], the molecular $D^*D_1(D_1')$ state [13, 14, 15, 16, 17, 18, 19, 20], the tetraquark state [21, 22, 23, 24, 25, 26], the cusp in the D^*D_1 channel [27], the radially excited state of the D_s [28], the pseudo-resonance structure [29], etc.

In Refs.[30, 31], we assume that the hidden charmed mesons $Z(4050)$ and $Z(4250)$ are vector (and scalar) tetraquark states, and study their masses using the QCD sum rules. The numerical results indicate that the mass of the vector hidden charmed tetraquark state is about $M_Z = (5.12 \pm 0.15)$ GeV or (5.16 ± 0.16) GeV, while the mass of the scalar hidden charmed tetraquark state is about $M_Z = (4.36 \pm 0.18)$ GeV. The resonance-like structure $Z(4250)$ observed by the Belle collaboration in the exclusive decays $\bar{B}^0 \rightarrow K^-\pi^+\chi_{c1}$ can

¹E-mail, wangzgyiti@yahoo.com.cn.

²There have been many theoretical works on the X , Y , Z hadrons, it is difficult to cite all of them, we prefer the comprehensive review articles [1, 2, 3, 4, 5], where one can find the original literatures. On the other hand, one can consult Ref.[6] for a concise review of the experimental situation of the new charmonium-like states.

be tentatively identified as the scalar tetraquark state [31]. In Refs.[32, 33], we study the mass spectrum of the scalar hidden charmed and hidden bottom tetraquark states in a systematic way using the QCD sum rules. In Ref.[34], we study the mass spectrum of the vector hidden charmed and hidden bottom tetraquark states systematically. Recently, the 0^{--} hidden charmed and hidden bottom tetraquark states are studied with the QCD sum rules [35].

In this article, we extend our previous works to study the mass spectrum of the axial-vector hidden charmed and hidden bottom tetraquark states in a systematic way with the QCD sum rules, and make possible explanation for the nature of the $Z^+(4430)$. The mass is a fundamental parameter in describing a hadron, whether or not there exist those hidden charmed or hidden bottom tetraquark configurations is of great importance itself, because it provides a new opportunity for a deeper understanding of the low energy QCD. The axial-vector hidden charmed ($c\bar{c}$) and hidden bottom ($b\bar{b}$) tetraquark states may be observed at the LHCb, where the $b\bar{b}$ pairs will be copiously produced with the cross section about $500 \mu b$ [36].

The hidden charmed and hidden bottom tetraquark states (denoted as Z) have the symbolic quark structures:

$$\begin{aligned} Z^+ &= Q\bar{Q}u\bar{d}; & Z^0 &= \frac{1}{\sqrt{2}}Q\bar{Q}(u\bar{u} - d\bar{d}); & Z^- &= Q\bar{Q}d\bar{u}; \\ Z_s^+ &= Q\bar{Q}u\bar{s}; & Z_s^- &= Q\bar{Q}s\bar{u}; & Z_s^0 &= Q\bar{Q}d\bar{s}; & \bar{Z}_s^0 &= Q\bar{Q}s\bar{d}; \\ Z_\varphi &= \frac{1}{\sqrt{2}}Q\bar{Q}(u\bar{u} + d\bar{d}); & Z_\phi &= Q\bar{Q}s\bar{s}, \end{aligned} \quad (1)$$

where the Q denote the heavy quarks c and b .

We take the diquarks as the basic constituents following Jaffe and Wilczek [37, 38], and construct the axial-vector tetraquark states with the diquark and antidiquark pairs. The diquarks have five Dirac tensor structures, scalar $C\gamma_5$, pseudoscalar C , vector $C\gamma_\mu\gamma_5$, axial-vector $C\gamma_\mu$ and tensor $C\sigma_{\mu\nu}$, where C is the charge conjugation matrix. The structures $C\gamma_\mu$ and $C\sigma_{\mu\nu}$ are symmetric, the structures $C\gamma_5$, C and $C\gamma_\mu\gamma_5$ are antisymmetric. The attractive interactions of one-gluon exchange favor formation of the diquarks in color antitriplet $\bar{3}_c$, flavor antitriplet $\bar{3}_f$ and spin singlet 1_s [39, 40]. In this article, we assume the axial-vector hidden charmed and hidden bottom tetraquark states Z consist of the $C\gamma_5 - C\gamma_\mu$ type rather than $C - C\gamma_\mu\gamma_5$ type diquark structures, and construct the interpolating currents $J^\mu(x)$ and $\eta^\mu(x)$:

$$\begin{aligned} J_{Z^+}^\mu(x) &= \epsilon^{ijk}\epsilon^{imn}u_j^T(x)C\gamma_5Q_k(x)\bar{Q}_m(x)\gamma^\mu C\bar{d}_n^T(x), \\ J_{Z^0}^\mu(x) &= \frac{\epsilon^{ijk}\epsilon^{imn}}{\sqrt{2}}[u_j^T(x)C\gamma_5Q_k(x)\bar{Q}_m(x)\gamma^\mu C\bar{u}_n^T(x) - (u \rightarrow d)], \\ J_{Z_s^+}^\mu(x) &= \epsilon^{ijk}\epsilon^{imn}u_j^T(x)C\gamma_5Q_k(x)\bar{Q}_m(x)\gamma^\mu C\bar{s}_n^T(x), \\ J_{Z_s^0}^\mu(x) &= \epsilon^{ijk}\epsilon^{imn}d_j^T(x)C\gamma_5Q_k(x)\bar{Q}_m(x)\gamma^\mu C\bar{s}_n^T(x), \\ J_{Z_\varphi}^\mu(x) &= \frac{\epsilon^{ijk}\epsilon^{imn}}{\sqrt{2}}[u_j^T(x)C\gamma_5Q_k(x)\bar{Q}_m(x)\gamma^\mu C\bar{u}_n^T(x) + (u \rightarrow d)], \\ J_{Z_\phi}^\mu(x) &= \epsilon^{ijk}\epsilon^{imn}s_j^T(x)C\gamma_5Q_k(x)\bar{Q}_m(x)\gamma^\mu C\bar{s}_n^T(x), \end{aligned} \quad (2)$$

$$\begin{aligned}
\eta_{Z^+}^\mu(x) &= \epsilon^{ijk} \epsilon^{imn} u_j^T(x) C \gamma^\mu Q_k(x) \bar{Q}_m(x) \gamma_5 C \bar{d}_n^T(x), \\
\eta_{Z^0}^\mu(x) &= \frac{\epsilon^{ijk} \epsilon^{imn}}{\sqrt{2}} [u_j^T(x) C \gamma^\mu Q_k(x) \bar{Q}_m(x) \gamma_5 C \bar{u}_n^T(x) - (u \rightarrow d)], \\
\eta_{Z_s^+}^\mu(x) &= \epsilon^{ijk} \epsilon^{imn} u_j^T(x) C \gamma^\mu Q_k(x) \bar{Q}_m(x) \gamma_5 C \bar{s}_n^T(x), \\
\eta_{Z_s^0}^\mu(x) &= \epsilon^{ijk} \epsilon^{imn} d_j^T(x) C \gamma^\mu Q_k(x) \bar{Q}_m(x) \gamma_5 C \bar{s}_n^T(x), \\
\eta_{Z_\varphi}^\mu(x) &= \frac{\epsilon^{ijk} \epsilon^{imn}}{\sqrt{2}} [u_j^T(x) C \gamma^\mu Q_k(x) \bar{Q}_m(x) \gamma_5 C \bar{u}_n^T(x) + (u \rightarrow d)], \\
\eta_{Z_\phi}^\mu(x) &= \epsilon^{ijk} \epsilon^{imn} s_j^T(x) C \gamma^\mu Q_k(x) \bar{Q}_m(x) \gamma_5 C \bar{s}_n^T(x),
\end{aligned} \tag{3}$$

where the i, j, k, \dots are color indexes. In the isospin limit, the interpolating currents result in three distinct expressions for the spectral densities, which are characterized by the number of the s quark they contain. The interpolating currents $J^\mu(x)$ and $\eta^\mu(x)$ lead to the same expression for the correlation functions $\Pi_{\mu\nu}(p)$, for example,

$$\begin{aligned}
J_{Z^+}^\mu &\sim \eta_{Z^+}^\mu; & J_{Z^0}^\mu &\sim \eta_{Z^0}^\mu; & J_{Z^-}^\mu &\sim \eta_{Z^-}^\mu; \\
J_{Z_s^+}^\mu &\sim \eta_{Z_s^+}^\mu; & J_{Z_s^-}^\mu &\sim \eta_{Z_s^-}^\mu; & J_{Z_s^0}^\mu &\sim \eta_{Z_s^0}^\mu; & J_{\bar{Z}_s^+}^\mu &\sim \eta_{\bar{Z}_s^+}^\mu; \\
J_{Z_\varphi}^\mu &\sim \eta_{Z_\varphi}^\mu; & J_{Z_\phi}^\mu &\sim \eta_{Z_\phi}^\mu,
\end{aligned} \tag{4}$$

where we use \sim to denote the two interpolating currents lead to the same expression. The special superpositions $tJ^\mu(x) + (1-t)\eta^\mu(x)$ can't improve the predictions remarkably, where $t = 0 - 1$. In this article, we take the interpolating currents $J^\mu(x)$ for simplicity, i.e. $t = 1$.

In fact, we can take the colored diquarks as point particles and describe them with the scalar S^a , pseudoscalar P^a , vector V_μ^a , axial-vector A_μ^a and tensor $T_{\mu\nu}^a$ fields, respectively, where the a is the color index, then introduce the $SU(3)$ color interaction. We construct the color singlet tetraquark currents with the diquark fields $S^a, P^a, V_\mu^a, A_\mu^a$ and $T_{\mu\nu}^a$, parameterize the nonperturbative effects with the new vacuum condensates $\langle \bar{S}S \rangle, \langle \bar{P}P \rangle, \langle \bar{V}V \rangle, \langle \bar{A}A \rangle$ and $\langle \bar{T}T \rangle$ besides the gluon condensate, and perform the standard procedure of the QCD sum rules to study the tetraquark states. The basic parameters such as the diquark masses and the new vacuum condensates can be fitted phenomenally. The nonet scalar mesons below 1 GeV (the $f_0(980)$ and $a_0(980)$ especially) are good candidates for the tetraquark states, from those tetraquark candidates, we can obtain the basic parameters and extend the new sum rules to other tetraquark states. As there are many works to do, we prefer another article.

The article is arranged as follows: we derive the QCD sum rules for the axial-vector hidden charmed and hidden bottom tetraquark states Z in Sect.2; in Sect.3, we present the numerical results and discussions; and Sect.4 is reserved for our conclusions.

2 QCD sum rules for the axial-vector tetraquark states Z

In the following, we write down the two-point correlation functions $\Pi_{\mu\nu}(p)$ in the QCD sum rules,

$$\Pi_{\mu\nu}(p) = i \int d^4x e^{ip \cdot x} \langle 0 | T [J_\mu(x) J_\nu^\dagger(0)] | 0 \rangle, \quad (5)$$

where the $J^\mu(x)$ denotes the interpolating currents $J_{Z^+}^\mu(x)$, $J_{Z^0}^\mu(x)$, $J_{Z_s^+}^\mu(x)$, etc.

We can insert a complete set of intermediate hadronic states with the same quantum numbers as the current operators $J_\mu(x)$ into the correlation functions $\Pi_{\mu\nu}(p)$ to obtain the hadronic representation [41, 42]. After isolating the ground state contribution from the pole term of the Z , we get the following result,

$$\Pi_{\mu\nu}(p) = \frac{\lambda_Z^2}{M_Z^2 - p^2} \left[-g_{\mu\nu} + \frac{p_\mu p_\nu}{p^2} \right] + \cdots, \quad (6)$$

where the pole residue (or coupling) λ_Z is defined by

$$\lambda_Z \epsilon_\mu = \langle 0 | J_\mu(0) | Z(p) \rangle, \quad (7)$$

the ϵ_μ denotes the polarization vector.

After performing the standard procedure of the QCD sum rules, we obtain the following six sum rules:

$$\lambda_Z^2 e^{-\frac{M_Z^2}{M^2}} = \int_{\Delta_Z}^{s_Z^0} ds \rho_Z(s) e^{-\frac{s}{M^2}}, \quad (8)$$

where the Z denote the channels $c\bar{c}q\bar{q}$, $c\bar{c}q\bar{s}$, $c\bar{c}s\bar{s}$, $b\bar{b}q\bar{q}$, $b\bar{b}q\bar{s}$ and $b\bar{b}s\bar{s}$ respectively; the s_Z^0 are the corresponding continuum threshold parameters, and the M^2 is the Borel parameter. The thresholds Δ_Z can be sorted into three sets, we introduce the $q\bar{q}$, $q\bar{s}$ and $s\bar{s}$ to denote the light quark constituents in the axial-vector tetraquark states to simplify the notation, $\Delta_{q\bar{q}} = 4m_Q^2$, $\Delta_{q\bar{s}} = (2m_Q + m_s)^2$, $\Delta_{s\bar{s}} = 4(m_Q + m_s)^2$. The explicit expressions of the spectral densities $\rho_{q\bar{q}}(s)$, $\rho_{q\bar{s}}(s)$ and $\rho_{s\bar{s}}(s)$ are presented in the appendix, where $\alpha_f = \frac{1 + \sqrt{1 - 4m_Q^2/s}}{2}$, $\alpha_i = \frac{1 - \sqrt{1 - 4m_Q^2/s}}{2}$, $\beta_i = \frac{\alpha m_Q^2}{\alpha s - m_Q^2}$, $\tilde{m}_Q^2 = \frac{(\alpha + \beta)m_Q^2}{\alpha\beta}$, $\tilde{\tilde{m}}_Q^2 = \frac{m_Q^2}{\alpha(1 - \alpha)}$.

We carry out the operator product expansion to the vacuum condensates adding up to dimension-10. In calculation, we take vacuum saturation for the high dimension vacuum condensates, they are always factorized to lower condensates with vacuum saturation in the QCD sum rules, factorization works well in large N_c limit. In reality, $N_c = 3$, some ambiguities may come from the vacuum saturation assumption.

We take into account the contributions from the quark condensates, mixed condensates, and neglect the contributions from the gluon condensate. The gluon condensate $\langle \frac{\alpha_s G G}{\pi} \rangle$ is of higher order in α_s , and its contributions are suppressed by very large denominators comparing with the four quark condensate $\langle \bar{q}q \rangle^2$ (or $\langle \bar{s}s \rangle^2$) and would not play any significant role, although the gluon condensate $\langle \frac{\alpha_s G G}{\pi} \rangle$ has smaller dimension of mass than the four quark condensate $\langle \bar{q}q \rangle^2$ (or $\langle \bar{s}s \rangle^2$). One can consult the sum rules for the light tetraquark states [43, 44], the heavy tetraquark state [31] and the heavy molecular states

[45, 46] for example. Furthermore, there are many terms involving the gluon condensate for the heavy tetraquark states and heavy molecular states in the operator product expansion (one can consult Refs.[31, 45]), we neglect the gluon condensate for simplicity.

In the special case of the $Y(4660)$ (as a $\psi' f_0(980)$ bound state) and its pseudoscalar partner $\eta'_c f_0(980)$, the contributions from the gluon condensate $\langle \frac{\alpha_s GG}{\pi} \rangle$ are rather large [47, 48]. If we take a simple replacement $\bar{s}(x)s(x) \rightarrow \langle \bar{s}s \rangle$ and $[\bar{u}(x)u(x) + \bar{d}(x)d(x)] \rightarrow 2\langle \bar{q}q \rangle$ in the interpolating currents, the standard heavy quark currents $Q(x)\gamma_\mu Q(x)$ and $Q(x)i\gamma_5 Q(x)$ are obtained, where the gluon condensate $\langle \frac{\alpha_s GG}{\pi} \rangle$ plays an important rule in the QCD sum rules [41]. The interpolating currents constructed from the diquark-antidiquark pairs do not have such feature. There are other interpretations for the $Y(4660)$, for example, the diquark-antidiquark type charmed baryonium [49].

We also neglect the terms proportional to the m_u and m_d , their contributions are of minor importance due to the small values of the u and d quark masses.

Differentiating the Eq.(8) with respect to $\frac{1}{M^2}$, then eliminate the pole residues λ_Z , we can obtain the sum rules for the masses of the Z ,

$$M_Z^2 = \frac{\int_{\Delta_Z}^{s_Z^0} ds \frac{d}{d(-1/M^2)} \rho_Z(s) e^{-\frac{s}{M^2}}}{\int_{\Delta_Z}^{s_Z^0} ds \rho_Z(s) e^{-\frac{s}{M^2}}} . \quad (9)$$

3 Numerical results and discussions

The input parameters are taken to be the standard values $\langle \bar{q}q \rangle = -(0.24 \pm 0.01 \text{ GeV})^3$, $\langle \bar{s}s \rangle = (0.8 \pm 0.2) \langle \bar{q}q \rangle$, $\langle \bar{q}g_s \sigma G q \rangle = m_0^2 \langle \bar{q}q \rangle$, $\langle \bar{s}g_s \sigma G s \rangle = m_0^2 \langle \bar{s}s \rangle$, $m_0^2 = (0.8 \pm 0.2) \text{ GeV}^2$, $m_s = (0.14 \pm 0.01) \text{ GeV}$, $m_c = (1.35 \pm 0.10) \text{ GeV}$ and $m_b = (4.8 \pm 0.1) \text{ GeV}$ at the energy scale $\mu = 1 \text{ GeV}$ [41, 42, 50].

The Q -quark masses appearing in the perturbative terms are usually taken to be the pole masses in the QCD sum rules, while the choice of the m_Q in the leading-order coefficients of the higher-dimensional terms is arbitrary [51, 52]. The \overline{MS} mass $m_c(m_c^2)$ relates with the pole mass \hat{m}_c through the relation $m_c(m_c^2) = \hat{m}_c \left[1 + \frac{C_F \alpha_s(m_c^2)}{\pi} + \dots \right]^{-1}$. In this article, we take the approximation $m_c(m_c^2) \approx \hat{m}_c$ without the α_s corrections for consistency. The value listed in the Particle Data Group is $m_c(m_c^2) = 1.27_{-0.11}^{+0.07} \text{ GeV}$ [53], it is reasonable to take $\hat{m}_c = m_c(1 \text{ GeV}^2) = (1.35 \pm 0.10) \text{ GeV}$. For the b quark, the \overline{MS} mass $m_b(m_b^2) = 4.20_{-0.07}^{+0.17} \text{ GeV}$ [53], the gap between the energy scale $\mu = 4.2 \text{ GeV}$ and 1 GeV is rather large, the approximation $\hat{m}_b \approx m_b(m_b^2) \approx m_b(1 \text{ GeV}^2)$ seems rather crude. It would be better to understand the quark masses m_c and m_b we take at the energy scale $\mu^2 = 1 \text{ GeV}^2$ as the effective quark masses (or just the mass parameters).

In calculation, we also neglect the contributions from the perturbative corrections. Those perturbative corrections can be taken into account in the leading logarithmic approximations through anomalous dimension factors. After the Borel transform, the effects of those corrections are to multiply each term on the operator product expansion side by the factor, $\left[\frac{\alpha_s(M^2)}{\alpha_s(\mu^2)} \right]^{2\Gamma_J - \Gamma_{\mathcal{O}_n}}$, where the Γ_J is the anomalous dimension of the interpolating current $J(x)$ and the $\Gamma_{\mathcal{O}_n}$ is the anomalous dimension of the local operator $\mathcal{O}_n(0)$. We carry out the operator product expansion at a special energy scale $\mu^2 = 1 \text{ GeV}^2$, and set the factor $\left[\frac{\alpha_s(M^2)}{\alpha_s(\mu^2)} \right]^{2\Gamma_J - \Gamma_{\mathcal{O}_n}} \approx 1$, such an approximation maybe result in some scale

dependence and weaken the prediction ability. In this article, we study the axial-vector hidden charmed and hidden bottom tetraquark states systemically, the predictions are still robust as we take the analogous criteria in those sum rules.

In the conventional QCD sum rules [41, 42], there are two criteria (pole dominance and convergence of the operator product expansion) for choosing the Borel parameter M^2 and threshold parameter s_0 . We impose the two criteria on the axial-vector heavy tetraquark states to choose the Borel parameter M^2 and threshold parameter s_0 .

The contributions from the high dimension vacuum condensates in the operator product expansion are shown in Figs.1-2, where (and thereafter) we use the $\langle\bar{q}q\rangle$ to denote the quark condensates $\langle\bar{q}q\rangle$, $\langle\bar{s}s\rangle$ and the $\langle\bar{q}g_s\sigma Gq\rangle$ to denote the mixed condensates $\langle\bar{q}g_s\sigma Gq\rangle$, $\langle\bar{s}g_s\sigma Gs\rangle$. From the figures, we can see that the contributions from the high dimension condensates are very large and change quickly with variation of the Borel parameter at the values $M^2 \leq 2.6 \text{ GeV}^2$ and $M^2 \leq 7.2 \text{ GeV}^2$ in the hidden charmed and hidden bottom channels respectively, such an unstable behavior cannot lead to stable sum rules, our numerical results confirm this conjecture, see Fig.4.

At the values $M^2 \geq 2.6 \text{ GeV}^2$ and $s_0 \geq 22 \text{ GeV}^2$, 23 GeV^2 , 23 GeV^2 , the contributions from the $\langle\bar{q}q\rangle^2 + \langle\bar{q}q\rangle\langle\bar{q}g_s\sigma Gq\rangle$ term are less than 12%, 5%, 2.5% in the channels $c\bar{c}q\bar{q}$, $c\bar{c}q\bar{s}$, $c\bar{c}s\bar{s}$ respectively; the contributions from the vacuum condensate of the highest dimension $\langle\bar{q}g_s\sigma Gq\rangle^2$ are less than 2.5%, 2%, 1.5% in the channels $c\bar{c}q\bar{q}$, $c\bar{c}q\bar{s}$, $c\bar{c}s\bar{s}$ respectively; we expect the operator product expansion is convergent in the hidden charmed channels.

At the values $M^2 \geq 7.2 \text{ GeV}^2$ and $s_0 \geq 136 \text{ GeV}^2$, 138 GeV^2 , 138 GeV^2 , the contributions from the $\langle\bar{q}q\rangle^2 + \langle\bar{q}q\rangle\langle\bar{q}g_s\sigma Gq\rangle$ term are less than 10%, 4.5%, 7% in the channels $b\bar{b}q\bar{q}$, $b\bar{b}q\bar{s}$, $b\bar{b}s\bar{s}$ respectively; the contributions from the vacuum condensate of the highest dimension $\langle\bar{q}g_s\sigma Gq\rangle^2$ are less than 5.5%, 4%, 3% in the channels $b\bar{b}q\bar{q}$, $b\bar{b}q\bar{s}$, $b\bar{b}s\bar{s}$ respectively; we expect the operator product expansion is convergent in the hidden bottom channels.

In this article, we take the uniform Borel parameter M_{min}^2 , i.e. $M_{min}^2 \geq 2.6 \text{ GeV}^2$ and $M_{min}^2 \geq 7.2 \text{ GeV}^2$ in the hidden charmed and hidden bottom channels respectively.

In Fig.3, we show the contributions from the pole terms with variation of the Borel parameters and the threshold parameters. The pole contributions are larger than (or equal) 46%, 50%, 50% at the value $M^2 \leq 3.2 \text{ GeV}^2$ and $s_0 \geq 22 \text{ GeV}^2$, 23 GeV^2 , 23 GeV^2 in the channels $c\bar{c}q\bar{q}$, $c\bar{c}q\bar{s}$, $c\bar{c}s\bar{s}$ respectively, and larger than (or equal) 48%, 50%, 50% at the value $M^2 \leq 8.2 \text{ GeV}^2$ and $s_0 \geq 136 \text{ GeV}^2$, 138 GeV^2 , 138 GeV^2 in the channels $b\bar{b}q\bar{q}$, $b\bar{b}q\bar{s}$, $b\bar{b}s\bar{s}$ respectively. Again we take the uniform Borel parameter M_{max}^2 , i.e. $M_{max}^2 \leq 3.2 \text{ GeV}^2$ and $M_{max}^2 \leq 8.2 \text{ GeV}^2$ in the hidden charmed and hidden bottom channels respectively.

In this article, the threshold parameters are taken as $s_0 = (23 \pm 1) \text{ GeV}^2$, $(24 \pm 1) \text{ GeV}^2$, $(24 \pm 1) \text{ GeV}^2$, $(138 \pm 2) \text{ GeV}^2$, $(140 \pm 2) \text{ GeV}^2$, $(140 \pm 2) \text{ GeV}^2$ in the channels $c\bar{c}q\bar{q}$, $c\bar{c}q\bar{s}$, $c\bar{c}s\bar{s}$, $b\bar{b}q\bar{q}$, $b\bar{b}q\bar{s}$, $b\bar{b}s\bar{s}$ respectively; the Borel parameters are taken as $M^2 = (2.6 - 3.2) \text{ GeV}^2$ and $(7.2 - 8.2) \text{ GeV}^2$ in the hidden charmed and hidden bottom channels respectively. In those regions, the pole contributions are about (46 - 74)%, (50 - 77)%, (50 - 77)%, (48 - 67)%, (50 - 69)%, (50 - 69)% in the channels $c\bar{c}q\bar{q}$, $c\bar{c}q\bar{s}$, $c\bar{c}s\bar{s}$, $b\bar{b}q\bar{q}$, $b\bar{b}q\bar{s}$, $b\bar{b}s\bar{s}$ respectively; the two criteria of the QCD sum rules are fully satisfied [41, 42].

From Fig.3, we can see that the Borel windows $M_{max}^2 - M_{min}^2$ change with variations of the threshold parameters s_0 . In this article, the Borel windows are taken as 0.6 GeV^2 and 1.0 GeV^2 in the hidden charmed and hidden bottom channels respectively; they are small

enough. If we take larger threshold parameters, the Borel windows are larger and the resulting masses are larger, see Fig.4. In this article, we intend to calculate the possibly lowest masses which are supposed to be the ground state masses by imposing the two criteria of the QCD sum rules.

If we take analogous pole contributions, the interpolating current with more s quarks requires slightly larger threshold parameter due to the $SU(3)$ breaking effects, see Fig.3. In the channels $Q\bar{Q}q\bar{s}$ and $Q\bar{Q}s\bar{s}$, the $SU(3)$ breaking effects on the threshold parameters are tiny, we take uniform threshold parameters in those channels. In Fig.4, we plot the axial-vector tetraquark state masses M_Z with variation of the Borel parameters and the threshold parameters. Naively, we expect the tetraquark state with more s quarks will have larger mass. In calculations, we observe that the possibly lowest masses of the axial-vector heavy tetraquark states $Q\bar{Q}q\bar{s}$ and $Q\bar{Q}s\bar{s}$ are almost the same.

Taking into account all uncertainties of the relevant parameters, finally we obtain the values of the masses and pole residues of the axial-vector tetraquark states Z , which are shown in Figs.5-6 and Table 1. In Table 1, we also present the masses of the scalar hidden charmed and hidden bottom tetraquark states obtained in our previous works [32, 33].

In this article, we calculate the uncertainties δ with the formula

$$\delta = \sqrt{\sum_i \left(\frac{\partial f}{\partial x_i} \right)^2 \Big|_{x_i=\bar{x}_i} (x_i - \bar{x}_i)^2}, \quad (10)$$

where the f denote the hadron mass M_Z and the pole residue λ_Z , the x_i denote the relevant parameters $m_c, m_b, \langle \bar{q}q \rangle, \langle \bar{s}s \rangle, \dots$. As the partial derivatives $\frac{\partial f}{\partial x_i}$ are difficult to carry out analytically, we take the approximation $\left(\frac{\partial f}{\partial x_i} \right)^2 (x_i - \bar{x}_i)^2 \approx [f(\bar{x}_i \pm \Delta x_i) - f(\bar{x}_i)]^2$ in the numerical calculations.

From Table 1, we can see that the uncertainties of the masses M_Z are rather small (about 4% in the hidden charmed channels and 2% in the hidden bottom channels), while the uncertainties of the pole residues λ_Z are rather large (about 20%). The uncertainties of the input parameters ($\langle \bar{q}q \rangle, \langle \bar{s}s \rangle, \langle \bar{s}g_s \sigma G s \rangle, \langle \bar{q}g_s \sigma G q \rangle, m_s, m_c$ and m_b) vary in the range (2–25)%, the uncertainties of the pole residues λ_Z are reasonable. We obtain the squared masses M_Z^2 through a fraction, the uncertainties in the numerator and denominator which originate from a given input parameter (for example, $\langle \bar{s}s \rangle, \langle \bar{s}g_s \sigma G s \rangle$) cancel out with each other, and result in small net uncertainty.

The $SU(3)$ breaking effects for the masses of the axial-vector hidden charmed and hidden bottom tetraquark states are buried in the uncertainties. Naively, we expect the axial-vector and vector diquarks have larger masses than the corresponding scalar diquarks, and the masses of the tetraquark states have the hierarchy $M_{C\gamma_\mu - C\gamma^\mu} \geq M_{C\gamma_5 - C\gamma^\mu} \geq M_{C\gamma_5 - C\gamma_5}$, because the attractive interactions of one-gluon exchange favor formation of the diquarks in color antitriplet $\bar{3}_c$, flavor antitriplet $\bar{3}_f$ and spin singlet 1_s [39, 40]. From Table 1, we can see that it is not the case.

In the conventional QCD sum rules, we usually consult the experimental data in choosing the Borel parameter M^2 and the threshold parameter s_0 . If the mass spectrum of the axial-vector tetraquark states are well known, we can denote the ground state, the first excited state, the second excited state, the third excited state, ..., as Z, Z', Z'', Z''', \dots . The critical thresholds for emergence of those excited tetraquark states are $T_{Z'}$,

$T_{Z''}, T_{Z'''}, \dots$, respectively. The threshold parameter s_0 should take values in the region $(M_Z + \Gamma_Z)^2 \leq s_0 < T_{Z'}$. However, the present experimental knowledge about the phenomenological hadronic spectral densities of the multiquark states is rather vague, even the existence of the multiquark states is not confirmed with confidence, and no knowledge about either there are high resonances or not.

Taking into account the two criteria (pole dominance and convergence of the operator product expansion) of the QCD sum rules, we can obtain the possibly lowest threshold parameter s_0 , which is denoted as s_{min}^0 . In this article, we take the value s_{min}^0 and make crude estimations for the ground state masses.

The values of the s_{min}^0 in different channels maybe smaller (or larger) than $T_{Z'}$, or even smaller than $(M_Z + \Gamma_Z)^2$, the two criteria of the QCD sum rules alone cannot always warrant satisfactory threshold parameters and Borel windows. For example, the nonet scalar mesons below 1 GeV (the $f_0(980)$ and $a_0(980)$ especially) are good candidates for the tetraquark states [38, 54, 55]. The two criteria of the QCD sum rules result in the threshold parameters $s_0 \gg (M_{f_0/a_0} + \Gamma_{f_0/a_0})^2$, the contributions of the excited states are already included in if there are any, and we have to resort to "multi-pole + continuum states" to approximate the phenomenological spectral densities. If we insist on the "one-pole + continuum states" ansatz, no reasonable Borel window can be obtained, although it is not an indication non-existence of the light tetraquark states (For detailed discussions about this subject, one can consult Refs.[31, 56]). The QCD sum rules is just a QCD model.

In the channel $c\bar{c}q\bar{q}$, the threshold parameter s_{min}^0 leads to the mass $M_{c\bar{c}q\bar{q}} = (4.32 \pm 0.18)$ GeV, which is consistent with the experimental data $M_Z = (4433 \pm 4 \pm 2)$ MeV or $4443_{-12}^{+15+19}_{-13}$ MeV from the Belle collaboration within uncertainty [7, 8]. The experimental value is $(M_Z + \Gamma_Z)^2 \leq 22.5 \text{ GeV}^2$, the lower bound of the $s_{min}^0 = (22 - 24) \text{ GeV}^2$ is smaller than $(M_Z + \Gamma_Z)^2$, we have to postpone the s_{min}^0 to larger values. If we take $s_0 = (26 \pm 1) \text{ GeV}^2$, the prediction $M_Z = (4.44 \pm 0.19)$ GeV is in excellent agreement with experimental data, see Fig.7. In Fig.8, we present the corresponding pole residue, from the figure, we can see that larger threshold parameter result in larger pole residue.

The predictions of the QCD sum rules favor the scenario of the $Z^+(4430)$ as an axial-vector tetraquark state, the $Z^+(4430)$ can be tentatively identified as an axial-vector tetraquark state. In other channels, the heavy axial-vector tetraquark states exist in nature maybe have larger masses than those theoretical predictions presented in Table 1. On the other hand, the upper bound of the threshold parameter $s_0 = (25 - 27) \text{ GeV}^2$ maybe larger than the critical threshold $T_{Z'}$, so we identify the $Z^+(4430)$ as an axial-vector tetraquark state tentatively, not confidently.

In Refs.[31, 32, 33], we observe that the meson $Z(4250)$ may be a scalar tetraquark state ($c\bar{c}u\bar{d}$), irrespective of the $C\gamma_\mu - C\gamma^\mu$ type and the $C\gamma_5 - C\gamma_5$ type diquark structures, the decay $Z(4250) \rightarrow \pi^+ \chi_{c1}$ can take place with the Okubo-Zweig-Iizuka super-allowed "fall-apart" mechanism, which can take into account the large total width naturally. In the present case, the decay $Z(4430) \rightarrow \psi' \pi$ can also take place with the Okubo-Zweig-Iizuka super-allowed "fall-apart" mechanism, which can take into account the large total width ($\Gamma_Z = 45_{-13}^{+18+30}_{-13}$ MeV or $107_{-43}^{+86+74}_{-56}$ MeV) naturally [7, 8].

In this article, we take the simple pole + continuum approximation for the phenomenological spectral densities. In fact, such a simple approximation has shortcomings. In the case of the non-relativistic harmonic-oscillator potential model, the spectrum of the bound

states (the masses E_n and the wave functions $\Psi_n(x)$) and the exact correlation functions (and hence its operator product expansion to any order) are known precisely. The non-relativistic harmonic-oscillator potential $\frac{1}{2}m\omega^2\vec{r}^2$ is highly non-perturbative, one suppose the full Green function satisfies the Lippmann-Schwinger operator equation and may be solved perturbatively. We can introduce the Borel parameter dependent effective threshold parameter $z_{eff}(M) = \omega [\bar{z}_0 + \bar{z}_1\sqrt{\frac{\omega}{M}} + \bar{z}_2\frac{\omega}{M} + \dots]$ and fit the coefficients \bar{z}_i to reproduce both the ground energy E_0 and the pole residue $R_0 = \Psi_0^*(0)\Psi_0(0)$, the phenomenological spectrum density can be described by the perturbative contributions well above the effective continuum threshold $z_{eff}(M)$, or reproduce the ground energy E_0 only and take the pole residue R as a calculated parameter, there exists a solution for the effective continuum threshold $z_{eff}(M)$ which precisely reproduces the exact ground energy E_0 for any value of the pole residue R within the range $R = (0.7 - 1.15)R_0$ in the limited fiducial Borel window, the value of the pole residue R extracted from the sum rule is determined to a great extent by the contribution of the hadron continuum [57]. There maybe systemic uncertainties out of control.

In the real QCD world, the hadronic spectral densities are not known exactly. In the present case, the ground states have not been observed yet, except for the possible axial-vector tetraquark state candidate $Z^+(4430)$. So we have no confidence to introduce the Borel parameter dependent effective threshold parameter $s_{eff}(M) = \bar{s}_0 + \bar{s}_1\frac{1}{M^2} + \bar{s}_2\frac{1}{M^4} + \dots$ and approximate the phenomenological spectral densities with the perturbative contributions above the effective continuum threshold $s_{eff}(M)$ accurately. Furthermore, the pole residues (or the couplings of the interpolating currents to the ground state tetraquark) λ_Z are not experimentally measurable quantities, and should be calculated by some theoretical approaches, the true values are difficult to obtain, which are distinguished from the decay constants of the pseudoscalar mesons and the vector mesons, the decay constants can be measured with great precision in the leptonic decays (in some channels).

The spectrum of the bound states in the non-relativistic harmonic-oscillator potential model are of the Dirac δ function type, we can choose $z_{eff} < E_1$, while in the case of the QCD, the situation is rather complex, the effective continuum thresholds $s_{eff}(M)$ maybe overlap with the first radial excited states, which are usually broad. For example, in the pseudoscalar channels, the widths of the π , $\pi(1300)$, $\pi(1800)$, \dots are ~ 0 GeV, $(0.2 - 0.6)$ GeV, (0.208 ± 0.012) GeV, \dots respectively, while the widths of the K , $K(1460)$, $K(1830)$, \dots are ~ 0 GeV, $\sim (0.25 - 0.26)$ GeV, ~ 0.25 GeV, \dots respectively [53]. In this article, we prefer (or have to choose) the simple pole + continuum approximation, and cannot estimate the unknown systemic uncertainties of the QCD sum rules before the spectral densities in both the QCD and phenomenological sides are known with great accuracy.

In Ref.[58], Lucha, Melikhov and Simula use the correlation function of the pseudoscalar current $J_5(x) = (m_b + m_u)\bar{q}(x)i\gamma_5 b(x)$ to illustrate a Borel-parameter-dependent effective continuum threshold can reduce considerably the (unphysical) dependence of the extracted bound-state mass and the decay constant on the Borel parameter. In the present case, we have no experimental data for the masses and pole residues of the tetraquark states to take as a guide and apply the χ^2 minimization by adjusting the effective threshold parameters. On the other hand, the Borel-parameter-dependent effective continuum thresholds maybe overlap with the $(M_Z + \Gamma_Z)^2$, $T_{Z'}$, $T_{Z''}$, \dots , we prefer the Borel-parameter-independent threshold parameters, although the Borel-parameter-dependent

effective threshold parameters maybe smear some dependence on the Borel parameter. From Figs.5-8, we can see that the dependence of the masses and pole residues on the Borel parameters in the Borel windows are rather mild.

The central values of our predictions are much larger than the corresponding ones from a relativistic quark model based on a quasipotential approach in QCD [59, 60]. In Refs.[59, 60], Ebert et al take the diquarks as bound states of the light and heavy quarks in the color antitriplet channel, and calculate their mass spectrum using a Schrodinger type equation, then take the masses of the diquarks as the basic input parameters, and study the mass spectrum of the heavy tetraquark states as bound states of the diquark-antidiquark system. In Refs.[61, 62, 63], Maiani et al take the diquarks as the basic constituents, examine the rich spectrum of the diquark-antidiquark states from the constituent diquark masses and the spin-spin interactions, and try to accommodate some of the newly observed charmonium-like resonances not fitting a pure $c\bar{c}$ assignment; furthermore, the corresponding bottom tetraquark states are also studied with the same method [64]. The predictions depend heavily on the assumption that the light scalar mesons $a_0(980)$ and $f_0(980)$ are tetraquark states, the basic parameters (constituent diquark masses) are estimated thereafter. In the conventional quark models, the constituent quark masses are taken as the basic input parameters, and fitted to reproduce the mass spectra of the conventional mesons and baryons. However, the present experimental knowledge about the phenomenological hadronic spectral densities of the tetraquark states is rather vague, whether or not there exist tetraquark states is not confirmed with confidence, and no knowledge about the high resonances. The predicted constituent diquark masses can not be confronted with the experimental data.

In Refs.[21, 60, 62], the $X(3872)$ and $Z(4430)$ are taken as the ground state axial-vector and first radially excited axial-vector tetraquark states respectively. In Ref.[65], Matheus et al study the $X(3872)$ as a tetraquark state with $J^{PC} = 1^{++}$ using QCD spectral sum rules, the prediction is consistent with the experimental data within uncertainty. The discrepancy between the predictions of Ref.[65] and the present work (analogous interpolating currents are chosen in those works) mainly originates from the high dimensional vacuum condensates $\langle \bar{q}g_s\sigma Gq \rangle^2$ which are neglected in Ref.[65]. The condensates $\langle \bar{q}g_s\sigma Gq \rangle^2$ are counted as $\mathcal{O}(\frac{m_c^6}{M^6})$, and the corresponding contributions are greatly enhanced at small M^2 , and result in rather bad convergent behavior in the operator product expansion, we have to choose larger Borel parameter M^2 . We insist on taking into account the high dimensional vacuum condensates, as the interpolating current consists of a light quark-antiquark pair and a heavy quark-antiquark pair, one of the highest dimensional vacuum condensates is $\langle \bar{q}q \rangle^2 \times \langle \frac{\alpha_s GG}{\pi} \rangle$, we have to take into account the condensates $\langle \bar{q}g_s\sigma Gq \rangle^2$ for consistence.

The LHCb is a dedicated b and c -physics precision experiment at the LHC (large hadron collider). The LHC will be the world's most copious source of the b hadrons, and a complete spectrum of the b hadrons will be available through gluon fusion. In proton-proton collisions at $\sqrt{s} = 14$ TeV, the $b\bar{b}$ cross section is expected to be $\sim 500\mu b$ producing 10^{12} $b\bar{b}$ pairs in a standard year of running at the LHCb operational luminosity of $2 \times 10^{32} \text{cm}^{-2}\text{sec}^{-1}$ [36]. The axial-vector tetraquark states predicted in the present work may be observed at the LHCb, if they exist indeed. We can search for the axial-vector hidden charm tetraquark states in the $D\bar{D}^*$, $D\bar{D}_s^*$, $D_s\bar{D}^*$, $D_s\bar{D}_s^*$, $J/\psi\pi$, $J/\psi K$, $J/\psi\eta$, $\psi'\pi$, $\psi'K$, \dots invariant mass distributions and search for the axial-vector hidden bottom tetraquark states in the $B\bar{B}^*$, $B\bar{B}_s^*$, $B_s\bar{B}^*$, $B_s\bar{B}_s^*$, $\Upsilon\pi$, ΥK , $\Upsilon\eta$, $\Upsilon'\pi$, $\Upsilon'K$, $\Upsilon'\eta$,

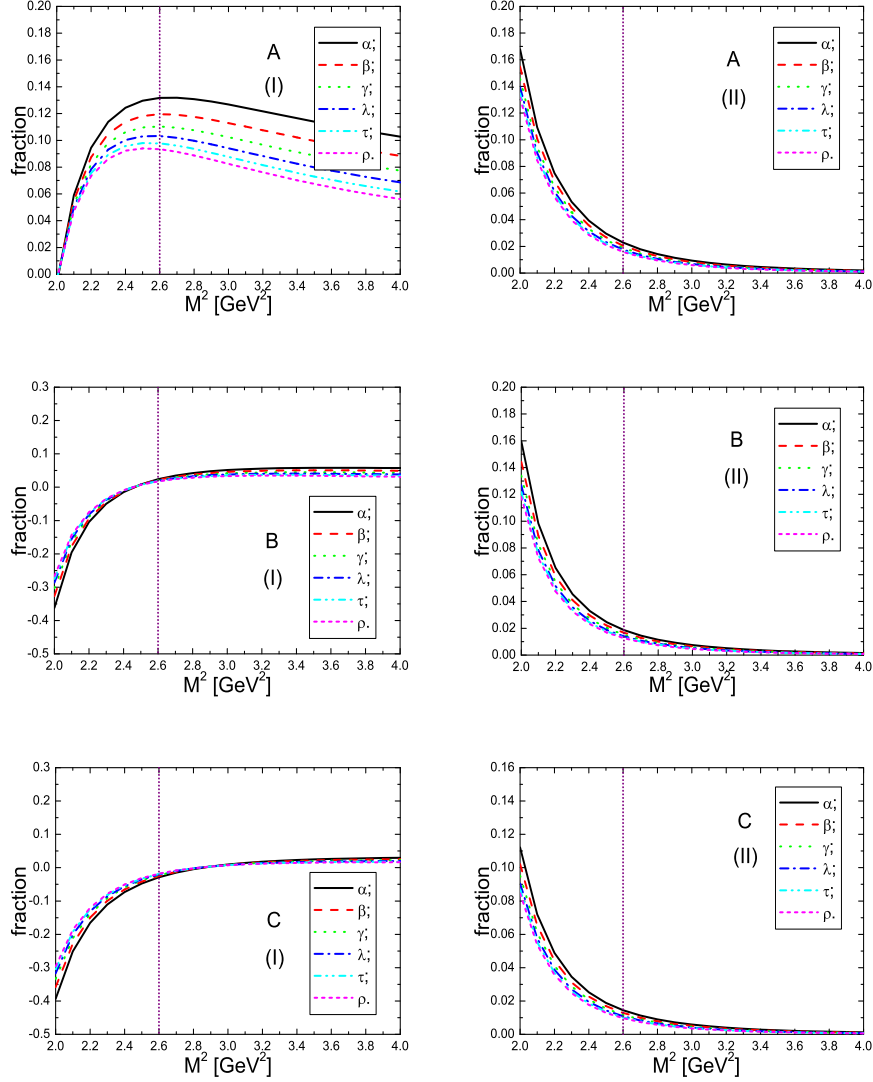


Figure 1: The contributions from different terms with variation of the Borel parameter M^2 in the operator product expansion. The (I) and (II) denote the contributions from the $\langle \bar{q}q \rangle^2 + \langle \bar{q}q \rangle \langle \bar{q}g_s \sigma Gq \rangle$ term and the $\langle \bar{q}g_s \sigma Gq \rangle^2$ term respectively. The A, B and C denote the channels $c\bar{c}q\bar{q}$, $c\bar{c}q\bar{s}$ and $c\bar{c}s\bar{s}$ respectively. The notations α , β , γ , λ , τ and ρ correspond to the threshold parameters $s_0 = 21 \text{ GeV}^2$, 22 GeV^2 , 23 GeV^2 , 24 GeV^2 , 25 GeV^2 and 26 GeV^2 respectively.

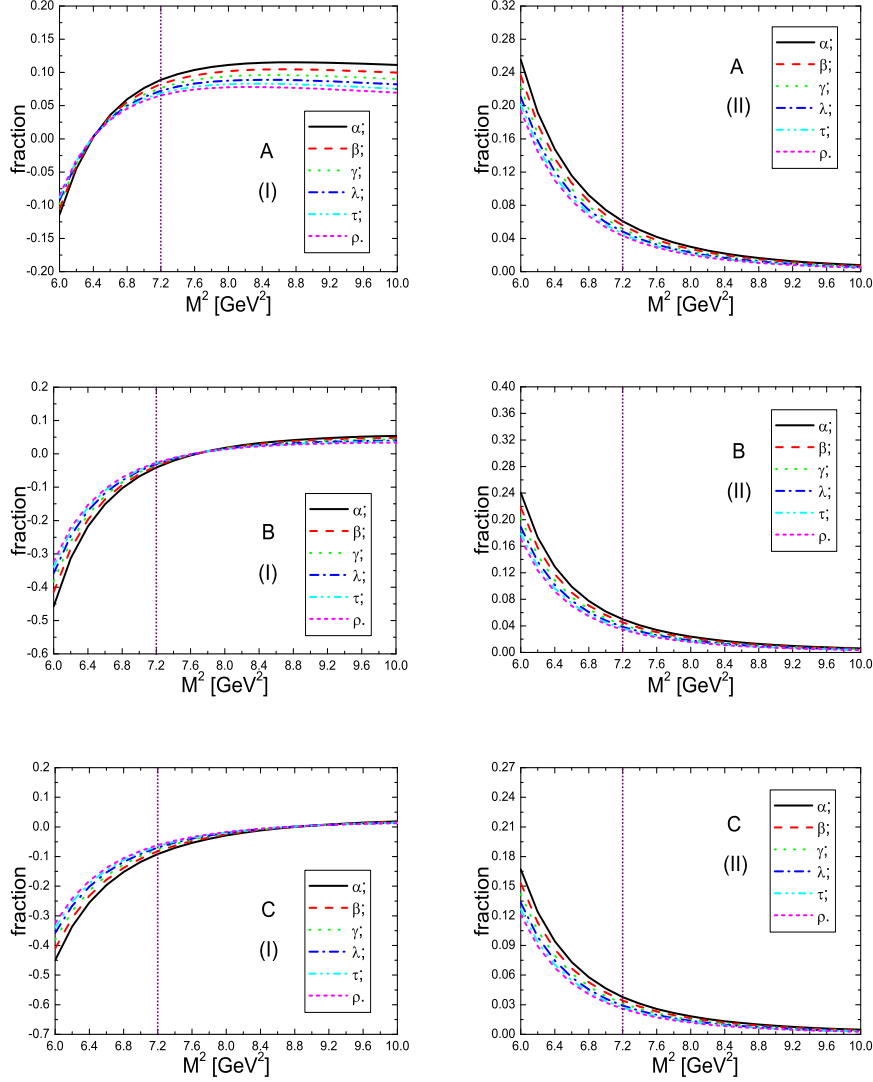


Figure 2: The contributions from different terms with variation of the Borel parameter M^2 in the operator product expansion. The (I) and (II) denote the contributions from the $\langle \bar{q}q \rangle^2 + \langle \bar{q}q \rangle \langle \bar{q}g_s \sigma Gq \rangle$ term and the $\langle \bar{q}g_s \sigma Gq \rangle^2$ term respectively. The A, B and C denote the channels $b\bar{b}q\bar{q}$, $b\bar{b}q\bar{s}$ and $b\bar{b}s\bar{s}$ respectively. The notations α , β , γ , λ , τ and ρ correspond to the threshold parameters $s_0 = 132 \text{ GeV}^2$, 134 GeV^2 , 136 GeV^2 , 138 GeV^2 , 140 GeV^2 and 142 GeV^2 respectively.

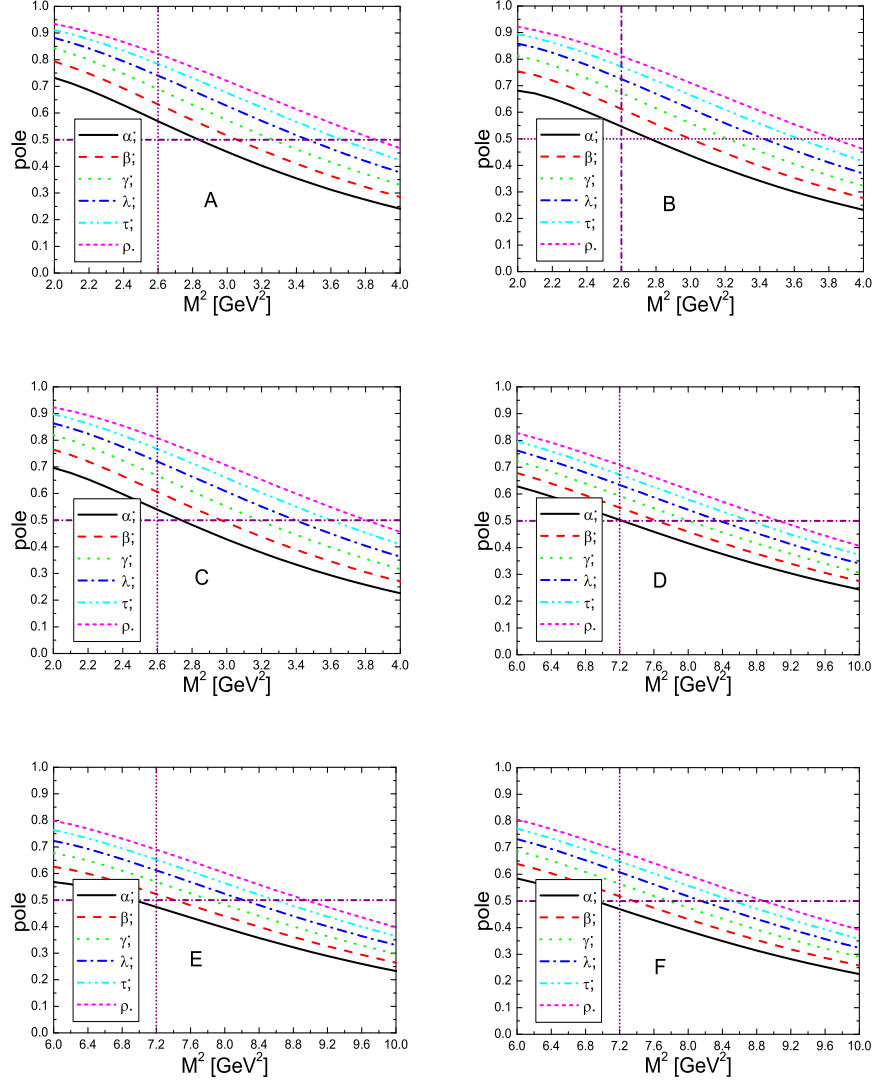


Figure 3: The contributions of the pole terms with variation of the Borel parameter M^2 . The A, B, C, D, E and F denote the channels $c\bar{c}q\bar{q}$, $c\bar{c}q\bar{s}$, $c\bar{c}s\bar{s}$, $b\bar{b}q\bar{q}$, $b\bar{b}q\bar{s}$ and $b\bar{b}s\bar{s}$ respectively. The notations α , β , γ , λ , τ and ρ correspond to the threshold parameters $s_0 = 21 \text{ GeV}^2$, 22 GeV^2 , 23 GeV^2 , 24 GeV^2 , 25 GeV^2 and 26 GeV^2 respectively in the hidden charmed channels; while they correspond to the threshold parameters $s_0 = 132 \text{ GeV}^2$, 134 GeV^2 , 136 GeV^2 , 138 GeV^2 , 140 GeV^2 and 142 GeV^2 respectively in the hidden bottom channels.

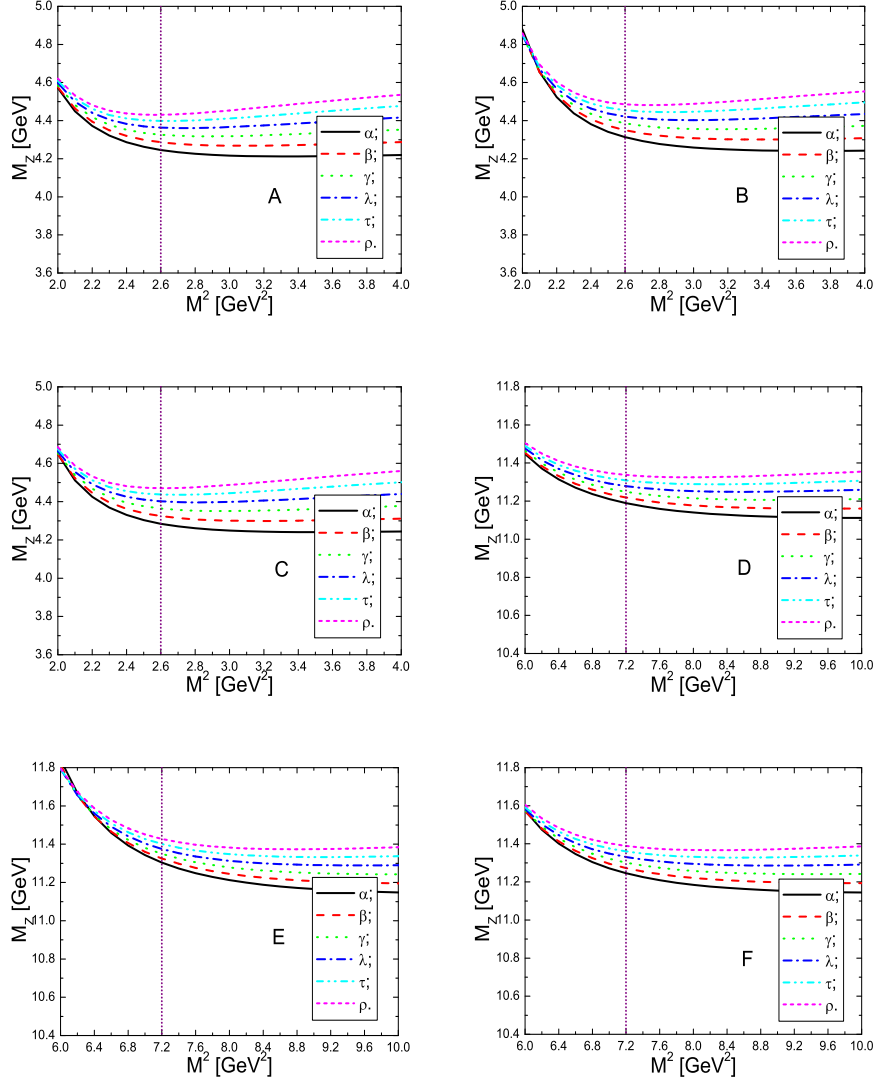


Figure 4: The masses of the axial-vector tetraquark states with variation of the Borel parameter M^2 . The A, B, C, D, E and F denote the channels $c\bar{c}q\bar{q}$, $c\bar{c}q\bar{s}$, $c\bar{c}s\bar{s}$, $b\bar{b}q\bar{q}$, $b\bar{b}q\bar{s}$ and $b\bar{b}s\bar{s}$ respectively. The notations α , β , γ , λ , τ and ρ correspond to the threshold parameters $s_0 = 21 \text{ GeV}^2$, 22 GeV^2 , 23 GeV^2 , 24 GeV^2 , 25 GeV^2 and 26 GeV^2 respectively in the hidden charmed channels; while they correspond to the threshold parameters $s_0 = 132 \text{ GeV}^2$, 134 GeV^2 , 136 GeV^2 , 138 GeV^2 , 140 GeV^2 and 142 GeV^2 respectively in the hidden bottom channels.

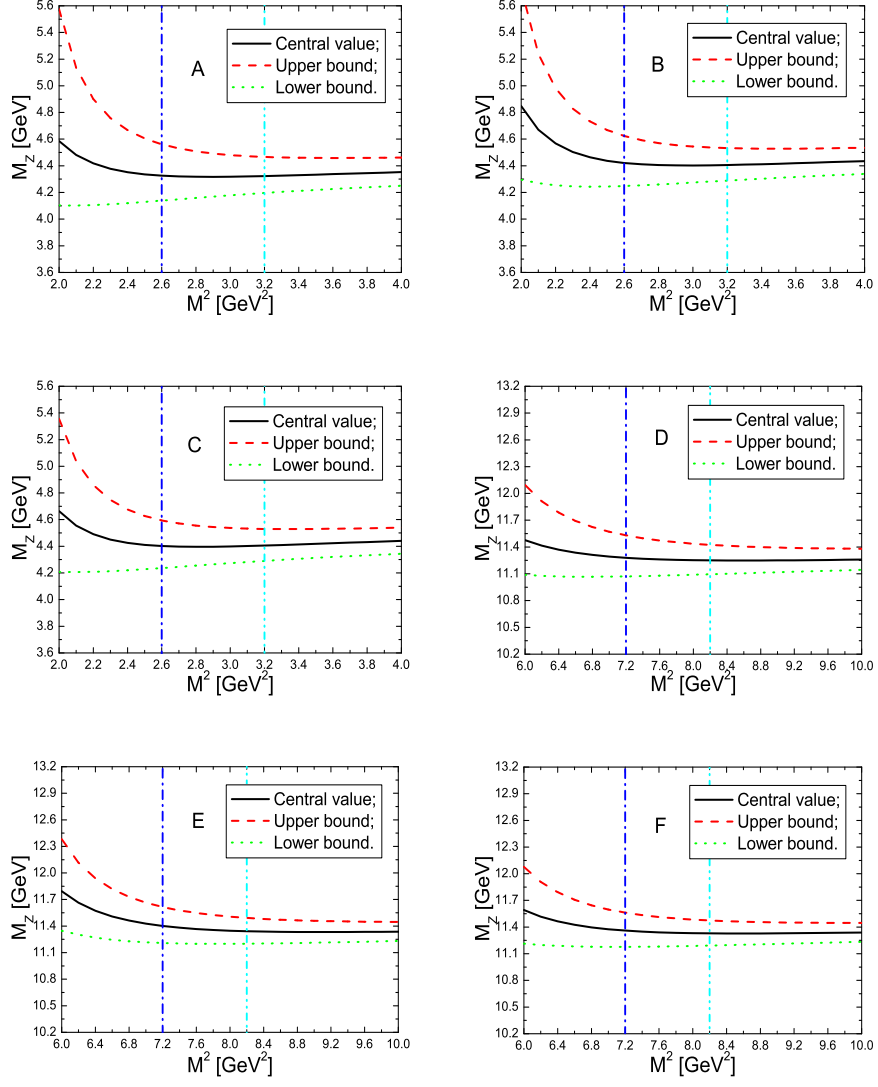


Figure 5: The masses of the axial-vector tetraquark states with variation of the Borel parameter M^2 . The A, B, C, D, E and F denote the channels $c\bar{c}q\bar{q}$, $c\bar{c}q\bar{s}$, $c\bar{c}s\bar{s}$, $b\bar{b}q\bar{q}$, $b\bar{b}q\bar{s}$ and $b\bar{b}s\bar{s}$ respectively.

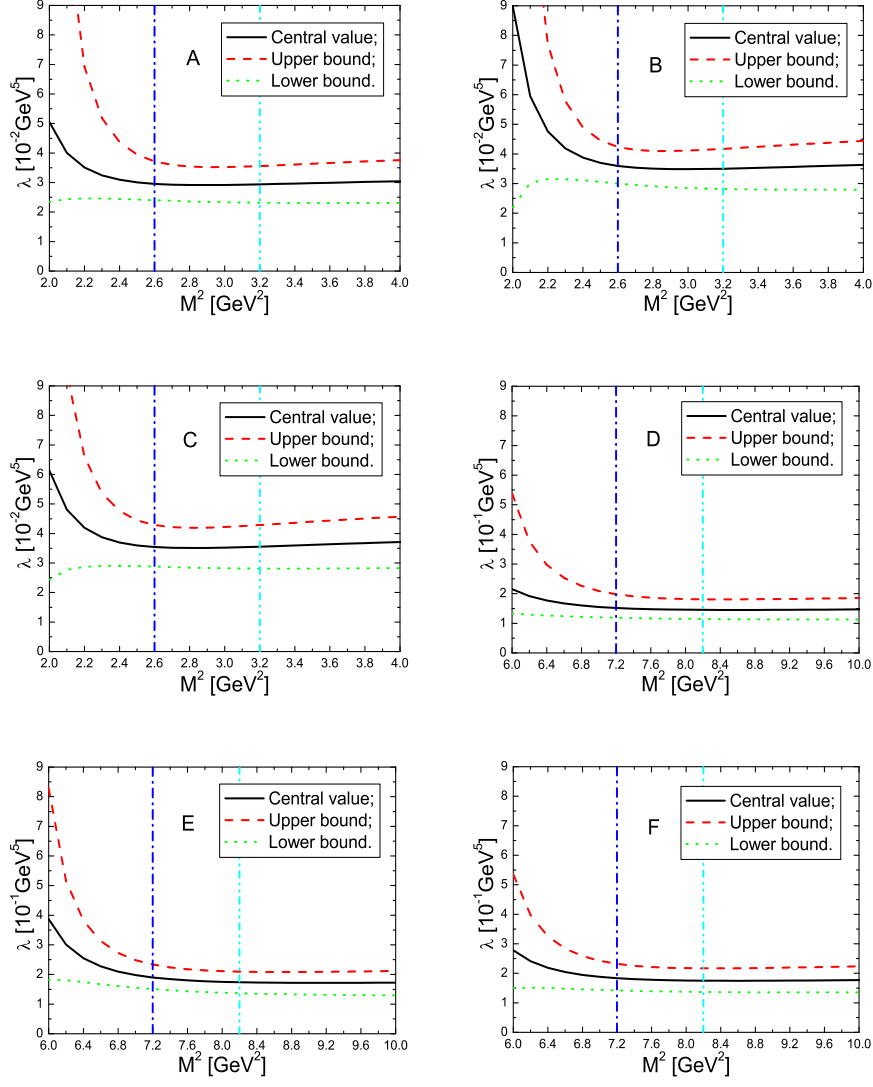


Figure 6: The pole residues of the axial-vector tetraquark states with variation of the Borel parameter M^2 . The A, B, C, D, E and F denote the channels $c\bar{c}q\bar{q}$, $c\bar{c}q\bar{s}$, $c\bar{c}s\bar{s}$, $b\bar{b}q\bar{q}$, $b\bar{b}q\bar{s}$ and $b\bar{b}s\bar{s}$ respectively.

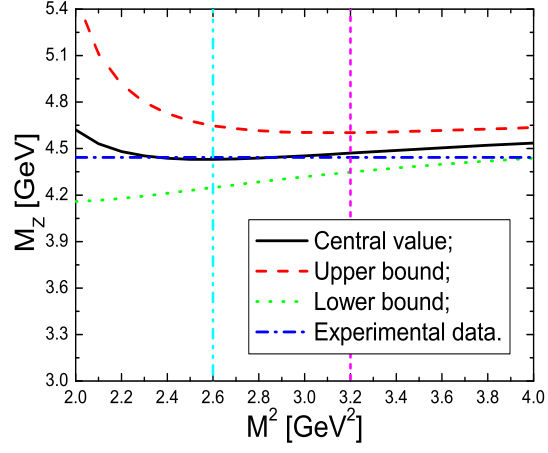


Figure 7: The mass of the $Z(4430)$ with variation of the Borel parameter M^2 .

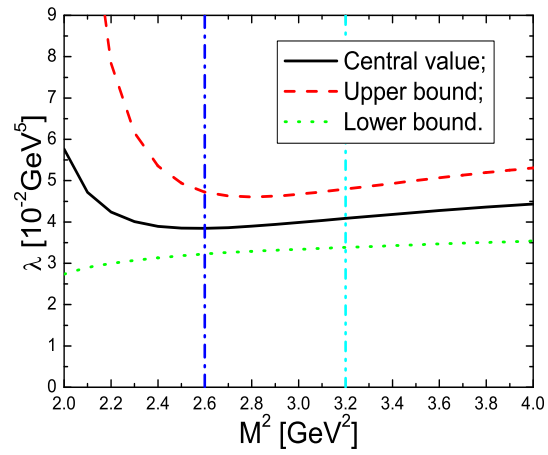


Figure 8: The pole residue of the $Z(4430)$ with variation of the Borel parameter M^2 .

tetraquark states	$C\gamma_5 - C\gamma_\mu$	λ_Z	$C\gamma_\mu - C\gamma^\mu$	$C\gamma_5 - C\gamma_5$
$c\bar{c}q\bar{q}$	4.32 ± 0.18	2.92 ± 0.60	4.36 ± 0.18	4.37 ± 0.18
$c\bar{c}q\bar{s}$	4.41 ± 0.16	3.51 ± 0.70		4.39 ± 0.16
$c\bar{c}s\bar{s}$	4.40 ± 0.16	3.51 ± 0.70	4.45 ± 0.16	4.44 ± 0.16
$b\bar{b}q\bar{q}$	11.27 ± 0.20	1.48 ± 0.34	11.14 ± 0.19	11.27 ± 0.20
$b\bar{b}q\bar{s}$	11.38 ± 0.18	1.80 ± 0.43		11.33 ± 0.16
$b\bar{b}s\bar{s}$	11.34 ± 0.16	1.78 ± 0.41	11.23 ± 0.16	11.31 ± 0.16
$Z(4430)$	4.44 ± 0.19	3.94 ± 0.71		

Table 1: The masses and the pole residues of the axial-vector tetraquark states. The masses are in unit of GeV and the pole residues are in unit of 10^{-2} GeV^5 and 10^{-1} GeV^5 in the channels $c\bar{c}$ and $b\bar{b}$ respectively.

... invariant mass distributions.

4 Conclusion

In this article, we construct the scalar-diquark-axial-vector-antidiquark type currents to interpolate the axial-vector tetraquark states, and study the mass spectrum of the axial-vector hidden charmed and hidden bottom tetraquark states with the QCD sum rules in a systematic way. In calculations, we take into account the contributions from the vacuum condensates adding up to dimension 10 in the operator product expansion, and neglect the gluon condensates as their contributions are supposed to be very small. The mass spectrum are calculated by imposing the two criteria (pole dominance and convergence of the operator product expansion) of the QCD sum rules. Our numerical result $M_{Z(4430)} = (4.44 \pm 0.19) \text{ GeV}$ is in excellent agreement with the experimental data $M_Z = (4433 \pm 4 \pm 2) \text{ MeV}$ or $4443_{-12}^{+15+19}_{-13} \text{ MeV}$ from the Belle collaboration, which indicates that the $Z^+(4430)$ can be identified as the axial-vector tetraquark state tentatively. Considering the light-flavor $SU(3)$ symmetry and the heavy quark symmetry, we make predictions for other axial-vector tetraquark states, the predictions can be confronted with the experimental data in the future at the LHCb or the Fermi-lab Tevatron.

Appendix

The spectral densities $\rho_{q\bar{q}}(s)$, $\rho_{q\bar{s}}(s)$ and $\rho_{s\bar{s}}(s)$ at the level of the quark-gluon degrees of freedom:

$$\begin{aligned}
\rho_{q\bar{q}}(s) = & \frac{1}{3072\pi^6} \int_{\alpha_i}^{\alpha_f} d\alpha \int_{\beta_i}^{1-\alpha} d\beta \alpha \beta (1-\alpha-\beta)^3 (s - \tilde{m}_Q^2)^2 (35s^2 - 26s\tilde{m}_Q^2 + 3\tilde{m}_Q^4) \\
& - \frac{m_Q \langle \bar{q}q \rangle}{32\pi^4} \int_{\alpha_i}^{\alpha_f} d\alpha \int_{\beta_i}^{1-\alpha} d\beta (1-\alpha-\beta) (s - \tilde{m}_Q^2) [(3\alpha + 4\beta)s - (\alpha + 2\beta)\tilde{m}_Q^2] \\
& + \frac{m_Q \langle \bar{q}g_s \sigma Gq \rangle}{64\pi^4} \int_{\alpha_i}^{\alpha_f} d\alpha \int_{\beta_i}^{1-\alpha} d\beta [(2\alpha + 3\beta)s - (\alpha + 2\beta)\tilde{m}_Q^2] \\
& + \frac{m_Q^2 \langle \bar{q}q \rangle^2}{12\pi^2} \int_{\alpha_i}^{\alpha_f} d\alpha - \frac{m_Q^2 \langle \bar{q}q \rangle \langle \bar{q}g_s \sigma Gq \rangle}{24\pi^2} \int_{\alpha_i}^{\alpha_f} d\alpha \left[1 + \frac{s}{M^2} \right] \delta(s - \tilde{m}_Q^2) \\
& + \frac{m_Q^2 \langle \bar{q}g_s \sigma Gq \rangle^2}{192\pi^2 M^6} \int_{\alpha_i}^{\alpha_f} d\alpha s^2 \delta(s - \tilde{m}_Q^2), \tag{11}
\end{aligned}$$

$$\begin{aligned}
\rho_{q\bar{s}}(s) = & \frac{1}{3072\pi^6} \int_{\alpha_i}^{\alpha_f} d\alpha \int_{\beta_i}^{1-\alpha} d\beta \alpha \beta (1-\alpha-\beta)^3 (s - \tilde{m}_Q^2)^2 (35s^2 - 26s\tilde{m}_Q^2 + 3\tilde{m}_Q^4) \\
& + \frac{m_s m_Q}{256\pi^6} \int_{\alpha_i}^{\alpha_f} d\alpha \int_{\beta_i}^{1-\alpha} d\beta \beta (1-\alpha-\beta)^2 (s - \tilde{m}_Q^2)^2 (5s - 2\tilde{m}_Q^2) \\
& + \frac{m_s \langle \bar{s}s \rangle}{64\pi^4} \int_{\alpha_i}^{\alpha_f} d\alpha \int_{\beta_i}^{1-\alpha} d\beta \alpha \beta (1-\alpha-\beta) (15s^2 - 16s\tilde{m}_Q^2 + 3\tilde{m}_Q^4) \\
& + \frac{m_Q \langle \bar{q}q \rangle}{32\pi^4} \int_{\alpha_i}^{\alpha_f} d\alpha \int_{\beta_i}^{1-\alpha} d\beta \alpha (1-\alpha-\beta) (s - \tilde{m}_Q^2) (\tilde{m}_Q^2 - 3s) \\
& + \frac{m_Q \langle \bar{s}s \rangle}{16\pi^4} \int_{\alpha_i}^{\alpha_f} d\alpha \int_{\beta_i}^{1-\alpha} d\beta \beta (1-\alpha-\beta) (s - \tilde{m}_Q^2) (\tilde{m}_Q^2 - 2s) \\
& + \frac{m_Q \langle \bar{q}g_s \sigma G q \rangle}{64\pi^4} \int_{\alpha_i}^{\alpha_f} d\alpha \int_{\beta_i}^{1-\alpha} d\beta \alpha (2s - \tilde{m}_Q^2) \\
& + \frac{m_Q \langle \bar{s}g_s \sigma G s \rangle}{64\pi^4} \int_{\alpha_i}^{\alpha_f} d\alpha \int_{\beta_i}^{1-\alpha} d\beta \beta (3s - 2\tilde{m}_Q^2) \\
& - \frac{m_s \langle \bar{s}g_s \sigma G s \rangle}{192\pi^4} \int_{\alpha_i}^{\alpha_f} d\alpha \int_{\beta_i}^{1-\alpha} d\beta \alpha \beta [8s - 3\tilde{m}_Q^2 + s^2 \delta(s - \tilde{m}_Q^2)] \\
& - \frac{m_s m_Q^2 \langle \bar{q}q \rangle}{16\pi^4} \int_{\alpha_i}^{\alpha_f} d\alpha \int_{\beta_i}^{1-\alpha} d\beta (s - \tilde{m}_Q^2) \\
& + \frac{m_Q^2 \langle \bar{q}q \rangle \langle \bar{s}s \rangle}{12\pi^2} \int_{\alpha_i}^{\alpha_f} d\alpha + \frac{m_s m_Q^2 \langle \bar{q}g_s \sigma G q \rangle}{64\pi^4} \int_{\alpha_i}^{\alpha_f} d\alpha \\
& - \frac{m_s m_Q \langle \bar{q}q \rangle \langle \bar{s}s \rangle}{24\pi^2} \int_{\alpha_i}^{\alpha_f} d\alpha \alpha [1 + s\delta(s - \tilde{m}_Q^2)] \\
& - \frac{m_Q^2 [\langle \bar{q}q \rangle \langle \bar{s}g_s \sigma G s \rangle + \langle \bar{s}s \rangle \langle \bar{q}g_s \sigma G q \rangle]}{48\pi^2} \int_{\alpha_i}^{\alpha_f} d\alpha \left[1 + \frac{s}{M^2} \right] \delta(s - \tilde{m}_Q^2) \\
& + \frac{m_s m_Q [2\langle \bar{q}q \rangle \langle \bar{s}g_s \sigma G s \rangle + 3\langle \bar{s}s \rangle \langle \bar{q}g_s \sigma G q \rangle]}{288\pi^2 M^2} \int_{\alpha_i}^{\alpha_f} d\alpha \alpha \left[s - \frac{s^2}{M^2} \right] \delta(s - \tilde{m}_Q^2) \\
& + \frac{m_Q^2 \langle \bar{q}g_s \sigma G q \rangle \langle \bar{s}g_s \sigma G s \rangle}{192\pi^2 M^6} \int_{\alpha_i}^{\alpha_f} d\alpha s^2 \delta(s - \tilde{m}_Q^2), \tag{12}
\end{aligned}$$

$$\begin{aligned}
\rho_{s\bar{s}}(s) = & \frac{1}{3072\pi^6} \int_{\alpha_i}^{\alpha_f} d\alpha \int_{\beta_i}^{1-\alpha} d\beta \alpha \beta (1-\alpha-\beta)^3 (s-\tilde{m}_Q^2)^2 (35s^2 - 26s\tilde{m}_Q^2 + 3\tilde{m}_Q^4) \\
& + \frac{m_s m_Q}{256\pi^6} \int_{\alpha_i}^{\alpha_f} d\alpha \int_{\beta_i}^{1-\alpha} d\beta (1-\alpha-\beta)^2 (s-\tilde{m}_Q^2)^2 [(4\alpha+5\beta)s - (\alpha+2\beta)\tilde{m}_Q^2] \\
& + \frac{m_s \langle \bar{s}s \rangle}{32\pi^4} \int_{\alpha_i}^{\alpha_f} d\alpha \int_{\beta_i}^{1-\alpha} d\beta \alpha \beta (1-\alpha-\beta) (15s^2 - 16s\tilde{m}_Q^2 + 3\tilde{m}_Q^4) \\
& - \frac{m_Q \langle \bar{s}s \rangle}{32\pi^4} \int_{\alpha_i}^{\alpha_f} d\alpha \int_{\beta_i}^{1-\alpha} d\beta (1-\alpha-\beta) (s-\tilde{m}_Q^2) [(3\alpha+4\beta)s - (\alpha+2\beta)\tilde{m}_Q^2] \\
& + \frac{m_Q \langle \bar{s}g_s \sigma G s \rangle}{64\pi^4} \int_{\alpha_i}^{\alpha_f} d\alpha \int_{\beta_i}^{1-\alpha} d\beta [(2\alpha+3\beta)s - (\alpha+2\beta)\tilde{m}_Q^2] \\
& - \frac{m_s \langle \bar{s}g_s \sigma G s \rangle}{96\pi^4} \int_{\alpha_i}^{\alpha_f} d\alpha \int_{\beta_i}^{1-\alpha} d\beta \alpha \beta [8s - 3\tilde{m}_Q^2 + s^2 \delta(s-\tilde{m}_Q^2)] \\
& - \frac{m_s m_Q^2 \langle \bar{s}s \rangle}{8\pi^4} \int_{\alpha_i}^{\alpha_f} d\alpha \int_{\beta_i}^{1-\alpha} d\beta (s-\tilde{m}_Q^2) \\
& + \frac{m_Q^2 \langle \bar{s}s \rangle^2}{12\pi^2} \int_{\alpha_i}^{\alpha_f} d\alpha + \frac{m_s m_Q^2 \langle \bar{s}g_s \sigma G s \rangle}{32\pi^4} \int_{\alpha_i}^{\alpha_f} d\alpha \\
& - \frac{m_s m_Q \langle \bar{s}s \rangle^2}{24\pi^2} \int_{\alpha_i}^{\alpha_f} d\alpha (1-\alpha) \left[2 + s\delta(s-\tilde{m}_Q^2) \right] \\
& - \frac{m_s m_Q \langle \bar{s}s \rangle^2}{24\pi^2} \int_{\alpha_i}^{\alpha_f} d\alpha \alpha \left[1 + s\delta(s-\tilde{m}_Q^2) \right] \\
& - \frac{m_Q^2 \langle \bar{s}s \rangle \langle \bar{s}g_s \sigma G s \rangle}{24\pi^2} \int_{\alpha_i}^{\alpha_f} d\alpha \left[1 + \frac{s}{M^2} \right] \delta(s-\tilde{m}_Q^2) \\
& + \frac{5m_s m_Q \langle \bar{s}s \rangle \langle \bar{s}g_s \sigma G s \rangle}{288\pi^2 M^2} \int_{\alpha_i}^{\alpha_f} d\alpha \alpha \left[s - \frac{s^2}{M^2} \right] \delta(s-\tilde{m}_Q^2) \\
& + \frac{5m_s m_Q \langle \bar{s}s \rangle \langle \bar{s}g_s \sigma G s \rangle}{144\pi^2} \int_{\alpha_i}^{\alpha_f} d\alpha (1-\alpha) \left[1 + \frac{s}{M^2} + \frac{s^2}{2M^4} \right] \delta(s-\tilde{m}_Q^2) \\
& + \frac{m_Q^2 \langle \bar{s}g_s \sigma G s \rangle^2}{192\pi^2 M^6} \int_{\alpha_i}^{\alpha_f} d\alpha s^2 \delta(s-\tilde{m}_Q^2), \tag{13}
\end{aligned}$$

Acknowledgements

This work is supported by National Natural Science Foundation of China, Grant Number 10775051, and Program for New Century Excellent Talents in University, Grant Number NCET-07-0282, and the Fundamental Research Funds for the Central Universities.

References

- [1] E. S. Swanson, Phys. Rept. **429** (2006) 243.

- [2] E. Klempt and A. Zaitsev, Phys. Rept. **454** (2007) 1.
- [3] M. B. Voloshin, Prog. Part. Nucl. Phys. **61** (2008) 455.
- [4] S. Godfrey and S. L. Olsen, Ann. Rev. Nucl. Part. Sci. **58** (2008) 51.
- [5] N. Drenska, R. Faccini, F. Piccinini, A. Polosa, F. Renga and C. Sabelli, arXiv:1006.2741.
- [6] S. L. Olsen, Nucl. Phys. **A827** (2009) 53C.
- [7] S. K. Choi et al, Phys. Rev. Lett. **100** (2008) 142001.
- [8] R. Mizuk et al, Phys. Rev. **D80** (2009) 031104.
- [9] B. Aubert et al, Phys. Rev. **D79** (2009) 112001.
- [10] R. Mizuk et al, Phys. Rev. **D78** (2008) 072004.
- [11] S. Dubynskiy and M. B. Voloshin, Phys. Lett. **B666** (2008) 344.
- [12] J. L. Rosner, Phys. Rev. **D76** (2007) 114002.
- [13] C. Meng and K. T. Chao, arXiv:0708.4222.
- [14] S. H. Lee, A. Mihara, F. S. Navarra and M. Nielsen, Phys. Lett. **B661** (2008) 28.
- [15] X. Liu, Y. R. Liu, W. Z. Deng and S. L. Zhu, Phys. Rev. **D77** (2008) 034003.
- [16] G. J. Ding, arXiv:0711.1485.
- [17] E. Braaten and M. Lu, Phys. Rev. **D79** (2009) 051503.
- [18] X. Liu, Y. R. Liu, W. Z. Deng and S. L. Zhu, Phys. Rev. **D77** (2008) 094015.
- [19] G. Z. Meng et al, Phys. Rev. **D80** (2009) 034503.
- [20] G. J. Ding, W. Huang, J. F. Liu and M. L. Yan, Phys. Rev. **D79** (2009) 034026.
- [21] L. Maiani, A. D. Polosa and V. Riquer, arXiv:0708.3997.
- [22] S. S. Gershtein, A. K. Likhoded and G. P. Pronko, arXiv:0709.2058.
- [23] Y. Li, C. D. Lu and W. Wang, Phys. Rev. **D77** (2008) 054001.
- [24] X. H. Liu, Q. Zhao and F. E. Close, Phys. Rev. **D77** (2008) 094005.
- [25] K. M. Cheung, W. Y. Keung and T. C. Yuan, Phys. Rev. **D76** (2007) 117501.
- [26] M. E. Bracco, S. H. Lee, M. Nielsen and R. Rodrigues da Silva, Phys. Lett. **B671** (2009) 240.
- [27] D. V. Bugg, arXiv:0709.1254.
- [28] T. Matsuki, T. Morii and K. Sudoh, Phys. Lett. **B669** (2008) 156.

- [29] I. V. Danilkin and P. Y. Kulikov, JETP Lett. **89** (2009) 390.
- [30] Z. G. Wang, Eur. Phys. J. **C59** (2009) 675.
- [31] Z. G. Wang, Eur. Phys. J. **C62** (2009) 375.
- [32] Z. G. Wang, Phys. Rev. **D79** (2009) 094027.
- [33] Z. G. Wang, Eur. Phys. J. **C67** (2010) 411.
- [34] Z. G. Wang, J. Phys. **G36** (2009) 085002.
- [35] W. Chen and S. L. Zhu, Phys. Rev. **D81** (2010) 105018.
- [36] G. Kane and A. Pierce, "Perspectives On LHC Physics", World Scientific Publishing Company, 2008.
- [37] R. L. Jaffe and F. Wilczek, Phys. Rev. Lett. **91** (2003) 232003.
- [38] R. L. Jaffe, Phys. Rept. **409** (2005) 1.
- [39] A. De Rujula, H. Georgi and S. L. Glashow, Phys. Rev. **D12** (1975) 147.
- [40] T. DeGrand, R. L. Jaffe, K. Johnson and J. E. Kiskis, Phys. Rev. **D12** (1975) 2060.
- [41] M. A. Shifman, A. I. Vainshtein and V. I. Zakharov, Nucl. Phys. **B147** (1979) 385.
- [42] L. J. Reinders, H. Rubinstein and S. Yazaki, Phys. Rept. **127** (1985) 1.
- [43] Z. G. Wang, Nucl. Phys. **A791** (2007) 106.
- [44] Z. G. Wang, W. M. Yang and S. L. Wan, J. Phys. **G31** (2005) 971.
- [45] Z. G. Wang, Eur. Phys. J. **C63** (2009) 115.
- [46] Z. G. Wang, Z. C. Liu and X. H. Zhang, Eur. Phys. J. **C64** (2009) 373.
- [47] Z. G. Wang and X. H. Zhang, Commun. Theor. Phys. **54** (2010) 323.
- [48] Z. G. Wang and X. H. Zhang, Eur. Phys. J. **C66** (2010) 419.
- [49] G. Cotugno, R. Faccini, A. D. Polosa and C. Sabelli, Phys. Rev. Lett. **104** (2010) 132005.
- [50] B. L. Ioffe, Prog. Part. Nucl. Phys. **56** (2006) 232.
- [51] S. Narison, Camb. Monogr. Part. Phys. Nucl. Phys. Cosmol. **17** (2002) 1.
- [52] A. Khodjamirian and R. Ruckl, Adv. Ser. Direct. High Energy Phys. **15** (1998) 345.
- [53] C. Amsler et al, Phys. Lett. **B667** (2008) 1.
- [54] F. E. Close and N. A. Tornqvist, J. Phys. **G28** (2002) R249.
- [55] C. Amsler and N. A. Tornqvist, Phys. Rept. **389** (2004) 61.

- [56] Z. G. Wang, Chin. Phys. **C32** (2008) 797.
- [57] W. Lucha, D. Melikhov and S. Simula, Phys. Rev. **D76** (2007) 036002.
- [58] W. Lucha, D. Melikhov and S. Simula, Phys. Lett. **B687** (2010) 48.
- [59] D. Ebert, R. N. Faustov and V. O. Galkin, Phys. Lett. **B634** (2006) 214.
- [60] D. Ebert, R. N. Faustov and V. O. Galkin, Eur. Phys. J. **C58** (2008) 399.
- [61] L. Maiani, F. Piccinini, A. D. Polosa and V. Riquer, Phys. Rev. Lett. **93** (2004) 212002.
- [62] L. Maiani, F. Piccinini, A. D. Polosa and V. Riquer, Phys. Rev. **D71** (2005) 014028.
- [63] N. V. Drenska, R. Faccini and A. D. Polosa, Phys. Rev. **D79** (2009) 077502.
- [64] A. Ali, C. Hambrock, I. Ahmed and M. Jamil Aslam, Phys. Lett. **B684** (2010) 28.
- [65] R. D. Matheus, S. Narison, M. Nielsen and J.M. Richard, Phys. Rev. **D75** (2007) 014005.